JOURNAL OF CATALYSIS 115, 441–451 (1989)

Acid and Catalytic Properties of Nonstoichiometric Aluminum Borates

KEVIN P. PEIL,* LAURINE G. GALYA,† AND GEORGE MARCELIN*,[1]

*Chemical and Petroleum Engineering Department, University of Pittsburgh, Pittsburgh, Pennsylvania 15261; and †University of Pittsburgh Applied Research Center, 100 William Pitt Way, Pittsburgh, Pennsylvania 15238

Received January 11, 1988; revised September 13, 1988

This paper details an investigation on the structure-acidity–catalytic activity relationship in aluminum borate mixed oxides. This aluminum borate mixed oxide is amorphous, is refractory, and exhibits properties which are dependent on the exact stoichiometry of the material. A series of catalysts with B/Al ratios ranging from 0 to 1 was prepared and characterized with respect to surface area, pore volume, and thermal stability. Nuclear magnetic resonance spectroscopy of ^{11}B and ^{27}Al was used to determine the local structure. Two boron species were identified: a tetrahedral BO_4 and a trigonal BO_3. The relative amounts of the two boron species were dependent on the B/Al stoichiometry. Three aluminum species were identified: a tetrahedral AlO_4, an octahedral AlO_6, and an AlO_4 with four B next-nearest neighbors. The strength and concentration of acid sites present on the surface of the aluminum borates were determined using adsorbed indicators. The presence and coordination of boron were seen to have a dramatic effect on the acidity of these materials with the acidity being closely related to the relative concentration of BO_4. 2-Propanol dehydration was used as a probe reaction to measure the acidity. Results from this reaction have shown these materials to indeed be highly acidic and catalytically active.

INTRODUCTION

Much work has been reported in the catalytic literature on the use of mixed oxides as both catalysts and catalytic supports (*1*). Mixed oxides, particularly alumina-based "binary oxides" such as silica–alumina and alumina–aluminum phosphate, are typically well suited catalytic materials because of their refractory nature, low cost, ability to be prepared with high surface area, ion exchange capacity, and physical durability. Recent work has shown that many of these properties are affected by the exact stoichiometry (relative amounts of the two cations) of the mixed oxide (*2–4*).

One important result of the reported mixed-oxide work is the knowledge that some of these materials can function as strong solid acids, some even behaving as superacids (*5*). Some compositions of silica–alumina and alumina–boria, for example, have been shown to have strong surface acidity (*6*). Acid catalysis is particularly important in a number of industrially important catalytic reactions, such as catalytic reforming, cracking, isomerization, alkylation, and dealkylation.

This paper reports recent investigations on the synthesis, chemical nature, and possible catalytic applications of mixed oxides consisting of Al_2O_3 and B_2O_3. Of particular interest was the relation between the structural nature of the materials and their chemical and catalytic properties.

EXPERIMENTAL

Preparation

The aluminum borate mixed oxides were prepared from common solutions of aluminum nitrate and boric acid using an ammonium hydroxide solution as a precipitant. The two solutions were slowly added into a third container of distilled water with the rate of addition controlled in order to main-

[1] To whom all correspondence should be addressed.

0021-9517/89 $3.00

tain a constant pH of 8. The resulting precipitate was filtered, washed with distilled water, oven-dried at 100°C overnight, and then later calcined at 500 or 1000°C for 4 to 6 hr. The samples were stored in air and used without any further pretreatment, except as indicated. The B/Al atomic ratios of the materials were varied from 0.05 to 1.0 by altering the relative amounts of aluminum nitrate and boric acid.

A stoichiometric shorthand notation will be used throughout this paper to indicate the varying atomic ratios of B/Al. For example, the mixed oxide of $3Al_2O_3 \cdot 2B_2O_3$ has a B/Al atomic ratio of 2/3 and is referred to simply as 3A2B.

Characterization

BET surface area and pore characteristics were obtained by nitrogen physisorption at −196°C using a Micromeritics 2600 surface area analyzer.

Differential thermal analysis (DTA) was carried out using a Perkin–Elmer 1700 DTA system over a temperature range from 25°C to approximately 1200°C. X-ray diffraction (XRD) analysis was performed using CuK_α radiation on samples calcined at both 500 and 1000°C. A General Electric Model 700 X-ray diffractometer was used. As will be shown later, the two calcination temperatures were chosen to bracket a characteristic exotherm indicated by DTA.

Acidity Measurements

The strength and concentration of the acidic sites present on the surface of the aluminum borate mixed oxide were measured using a modification of the method first outlined by Benesi (*6, 7*). The modification involved adding the *n*-butylamine solution directly to a catalyst sample containing an adsorbed indicator instead of the Benesi method of adding the indicator solution to a catalyst sample containing adsorbed *n*-butylamine.

Samples to be titrated were first dried at 300°C in a stream of flowing nitrogen. Since water can behave as a base and adsorb to the acidic surface sites, it is important that there be no water present during titration measurements. After drying, 0.1-g portions of catalyst were transferred to small screw cap vials and 2 g of isooctane was added to each of the vials. The entire procedure was carried out in a dry glovebox to ensure the absence of any water.

Several drops of each indicator solution (0.1%) were added to the capped suspensions of the sample to determine the strength of the strongest acid sites present. If an adsorbed indicator gave an acidic color, the sample was known to have acid sites of strength equal to or less than the H_0 of the adsorbed indicator. When an adsorbed indicator gave a basic color, no acidic sites with strength equal to or greater than the H_0 of that indicator were present. Reported values of H_0 correspond to the maximum strength of the strongest acid sites present.

To determine the total number of acidic sites present, each sample with an adsorbed indicator giving an acidic color was titrated with a 0.1 *M* *n*-butylamine solution. Approximately 1 to 2 min was allowed for the capped samples to equilibrate. When enough *n*-butylamine was added to remove the acidic color from the sample, the sample was said to have acidic sites less than or equal to the H_0 of the now removed indicator equal in number to the amount of *n*-butylamine added. Reported values of the total number of acid sites are for sites with an $H_0 \leq +1.5$ (*8*).

Nuclear Magnetic Resonance

^{11}B NMR spectra were taken of each of the samples calcined at 500 and 1000°C using a Bruker MSL-300 NMR spectrometer. The number of scans needed to ensure a high signal-to-noise ratio varied depending on the B/Al atomic ratio. For samples containing a small amount of ^{11}B (low B/Al), the number of scans taken varied from 1200 to 1400, whereby samples containing a high amount of ^{11}B (high B/Al) required only 16 scans. Magic-angle spinning (MAS) at

about 4 kHz was used during spectral acquisition.

All ^{11}B MAS NMR spectra were obtained at a ^{11}B NMR frequency of 96.25 MHz. All spectra were obtained using a <30° pulse width of 5 μs. Chemical shifts are reported in parts per million (ppm) on the basis of assigning the tetrahedrally coordinated ^{11}B peak in BPO_4 to 0 ppm. Background subtraction was necessary due to boron nitride components in the probe. Other parameters for obtaining the ^{11}B spectra were as follows: spectral width = 25 kHz, 1K data points in the time domain zero-filled to 4K data points in the frequency domain, filter width = 30 kHz, preacquisition delay = 7.5 μs, acquisition time = 20 ms, and line broadening factor = 50 Hz.

The ^{27}Al spectra were obtained at a ^{27}Al NMR frequency of 161 MHz. Chemical shifts are reported in ppm with the octahedrally coordinated ^{27}Al in γ-alumina assigned to 0 ppm. The parameters used for obtaining ^{27}Al spectra were as follows: 9° pulse width = 2.5μs, spinning rate = 4 kHz, spectral width = 100 kHz, 4K data points in the time domain zero-filled to 64K data points in the frequency domain, acquisition time = 150 ms, and line broadening factor = 150 Hz.

Catalytic Reaction Studies

The catalytic activity of these samples was investigated using 2-propanol dehydration as a test reaction. The reaction was carried out using 200 mg of catalyst in a fixed-bed system online with a gas chromatograph using a 50-m fused silica capillary column with crosslinked methyl silicone as the stationary phase. A saturator containing the 2-propanol was kept at a constant temperature of 40°C. Helium was used as a carrier gas and kept at a constant flow rate of 20 cc/min. Conversions were measured every 10° starting at approximately 150°C and continuing to approximately 200°C. From the conversions obtained, absolute rates and apparent activation energies were calculated.

RESULTS

Physical and Thermal Properties

Table 1 summarizes the chemical and structural characteristics of the aluminum borate mixed oxides prepared for this study. Listed in the table are the BET surface areas and cumulative pore volumes for samples calcined at 500°C, along with the particular crystalline phases detected by XRD after calcining each of the materials at 500 and 1000°C. Also given in the table are the corresponding properties for a similarly prepared Al_2O_3 previously reported (*9*).

Examination of the BET surface areas shows that the incorporation of boron into the alumina structure had little effect on either the specific surface area or the pore volume. Examination of the pore size distributions showed the lack of any bimodal pore distribution as would be expected for materials consisting of simply a mixture of two oxides, thereby indicating that these materials are not just mixtures of alumina and diboron trioxide.

Two exotherms were observed by DTA for all of the oven-dried aluminum borates occurring in two temperature ranges. A first exotherm occurred between 280 and 300°C

TABLE 1

Chemical and Structural Characteristics of Nonstoichiometric Aluminum Borate Mixed Oxides

Catalyst	B/Al	Surface area[a] (m^2/g)	Pore volume[a] (ml/g)	XRD phases calcination temperature	
				500°C	1000°C
Al_2O_3	0	302	0.320	γ-Al_2O_3	α-Al_2O_3 θ-Al_2O_3
20AB	0.05	306	0.503	Amorphous	γ-Al_2O_3
10AB	0.10	333	0.477	Am.	γ-Al_2O_3[b]
7AB	0.14	308	0.450	Am.	[b]
10A3B	0.30	307	0.437	Am.	[b]
2AB	0.50	250	0.572	Am.	2AB
3A2B	0.67	208	0.543	Am.	2AB
5A4B	0.80	176	0.457	Am.	2AB
1A1B	1.0	235	0.562	Am.	2AB

[a] After 500°C calcination.

[b] Weak signals showing the beginning of $2Al_2O_3 \cdot B_2O_3$ and $9Al_2O_3 \cdot 2B_2O_3$. Radiation source: Cu K_α.

and a second between 760 and 900°C. The first exotherm can be attributed to the initial formation of the oxide. In its oven-dried state, structural hydroxyls and surface water are still present. Upon heating of the samples, most of this structural and surface water is driven off until not enough water remains for the material to maintain its hydroxylated form, resulting in a restructuring to the oxide form.

The second exotherm can be attributed to the formation of a crystalline phase characteristic of aluminum borates with the equivalent chemical formula $2Al_2O_3 \cdot B_2O_3$ (*10*). The crystallization of $2Al_2O_3 \cdot B_2O_3$ from an amorphous phase and the decomposition of $2Al_2O_3 \cdot B_2O_3$ into $9Al_2O_3 \cdot 2B_2O_3$ have been previously studied and reported (*10*). The decomposition of $2Al_2O_3 \cdot B_2O_3$ into $9Al_2O_3 \cdot 2B_2O_3$ begins to occur at 1030°C. Some of the samples calcined at 1000°C showed in their XRD pattern weak signals corresponding to the $9Al_2O_3 \cdot 2B_2O_3$ phase, but in all cases the dominant phase was $2Al_2O_3 \cdot B_2O_3$.

One interesting feature of these aluminum borates was their continued amorphous nature after calcination at 500°C. Whereas upon calcination of Al_2O_3 at 500°C, the γ-Al_2O_3 phase is formed (*9*), even the aluminum borate containing the lowest amount of boron (the material with a B/Al of 1/20) maintained its amorphous nature after 500°C calcination. The γ-Al_2O_3 phase was formed in the materials containing a small amount of boron (B/Al = 1/20 and 1/10) only after calcination at 1000°C. No γ-Al_2O_3 was detected in any of the other samples after calcination at this temperature.

Short-Range Structure

Figure 1 shows the ^{11}B spectra of various model compounds and the characteristic signals arising from the two different coordinations common of ^{11}B. Boron phosphate (BPO_4) has all of the ^{11}B tetrahedrally coordinated with oxygen. Because of this tetrahedral coordination, the ^{11}B is in a highly symmetrical environment and its corresponding NMR signal is very sharp. The smaller signals sitting symmetrically on either side of the main tetrahedral peak at 0 ppm are the spinning sidebands and do not enter into the qualitative analysis of the spectra.

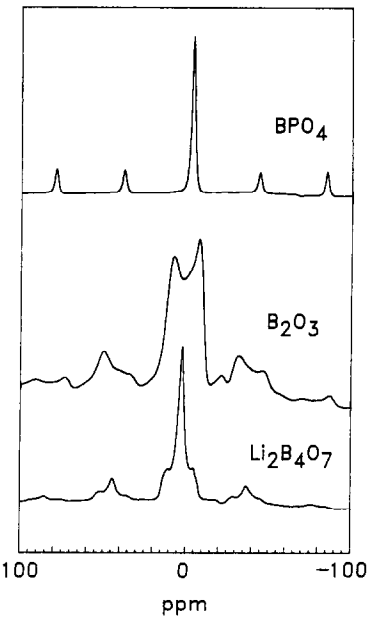

FIG. 1. ^{11}B characteristic NMR signals.

Diboron trioxide (B_2O_3), on the other hand, has all of its ^{11}B trigonally coordinated with oxygen. Because boron is a quadrupolar nucleus, quadrupolar splitting of the BO_3 signal ($e^2qQ/h \approx 2.5$ MHz (*11–13*)) which broadens and splits the NMR signal occurs, resulting in a signal which resembles a doublet. Unfortunately, the field strength used in this work resulted in overlap of the trigonal and tetrahedral signals, as illustrated by the last material shown in the figure, lithium borate ($Li_2B_4O_7$), which has a known trigonal/tetrahedral ratio of 1/1 (*14*). Despite this overlap, the trigonal and tetrahedral signals can be easily seen in the spectra and integrated.

Figures 2 and 3 show the ^{11}B NMR of the nonstoichiometric aluminum borates calcined at 500 and 1000°C, respectively. In

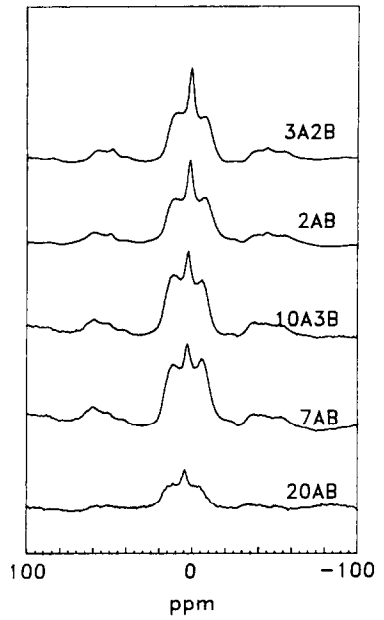

FIG. 2. ^{11}B NMR spectra of 500°C calcined aluminum borates.

all but one case, the nonstoichiometric aluminum borates were seen to consist of both trigonal and tetrahedral B–O coordinations. For the samples calcined at 500°C, a general pattern is observed of the tetrahedral signal intensity, and thus the tetrahedral coordination, increasing with increasing boron content. This is more evident from Fig. 4 which compares the integrated signals in terms of B_3/B_4 ratio. This figure is meant to show a trend rather than an absolute B_3/B_4 ratio. This is because the intensity of the tetrahedral signal will be higher than the signal intensity of an equivalent amount of trigonal boron. This intensity difference arises due to combined effects of the difference in the quadrupolar coupling constants of the two coordinations and the 30° pulse angle used.

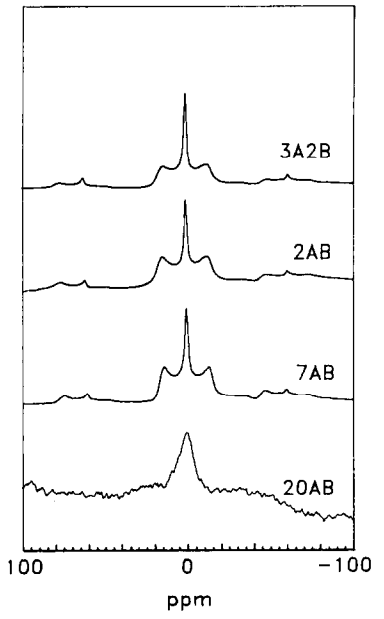

FIG. 3. ^{11}B NMR spectra of 1000°C calcined aluminum borates.

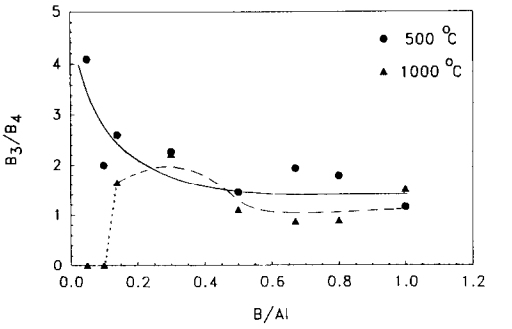

FIG. 4. Effect of B/Al ratio on B coordination: ●, 500°C calcined samples; ▲, 1000°C calcined samples.

A slightly different result was observed with the samples calcined at the higher temperature of 1000°C. When comparing the same sample calcined at the two different temperatures, the tetrahedral signal intensity increased relative to the trigonal signal with increasing calcination temperature. This was especially evident in the samples containing a small amount of boron. No trigonally coordinated ^{11}B was detected in the 1000°C calcined sample with a B/Al ratio equal to 0.05.

Figure 5 shows a typical ^{27}Al spectra of the 3A2B aluminum borate. Three different signals were observed in the spectra after calcination at 500°C. The signals at 1 and 62 ppm correspond respectively to the octahedral Al coordination, AlO_6, and the tetrahe-

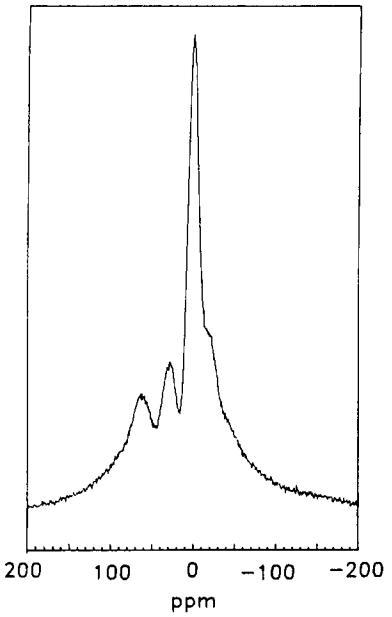

FIG. 5. ^{27}Al NMR spectra of 3A2B after calcination at 500°C.

dral coordination, AlO_4 (*15–20*). A third, smaller signal was also observed at about 30 ppm. Figure 6 shows the ^{27}Al spectra of the 3A2B aluminum borate after calcination at 1000°C, in which the 30 ppm signal was noted to increase and dominate the spectrum. There was also a considerable downfield shift of this signal. The signals corresponding to the octahedral and tetrahedral Al coordinations can be seen at 5 and 63 ppm, respectively.

Table 2 lists the chemical shifts of the major signals observed in the 500 and 1000°C calcined aluminum borates. In all cases, the highest upfield signal corresponding to octahedral Al fell within the reported range of chemical shifts of 0–20 ppm. The most downfield signal corresponding to tetrahedral Al was also within the reported range of chemical shifts of 50–80 ppm. In cases where a third signal was observed, it was in the chemical-shift range 25–45 ppm. Signals in this chemical-shift range are not common to either AlO_4 or AlO_6, but fall within the range reported for

TABLE 2

^{27}Al Apparent Chemical Shifts (ppm) for Nonstoichiometric Aluminum Borates

Sample	Calcination temp. (°C)	Major ^{27}Al signal chemical shifts (ppm)		
20AB	500	73	10	30
10A3B	500	71	6	30
5A4B	500	62	1	30
AB	500	65	1	25
20AB	1000	75	7	—
10A3B	1000	67	1	43
5A4B	1000	63	5	45
AB	1000	65	5	45

tetrahedral Al with four boron next-nearest neighbors, $Al(OB)_4$ (*21*). The signal was noted to move downfield by as much as 20 ppm with increasing calcination temperature and was absent for the 20AB sample. Comparatively, there was little change in chemical shifts for AlO_4 and AlO_6 with calcination temperature.

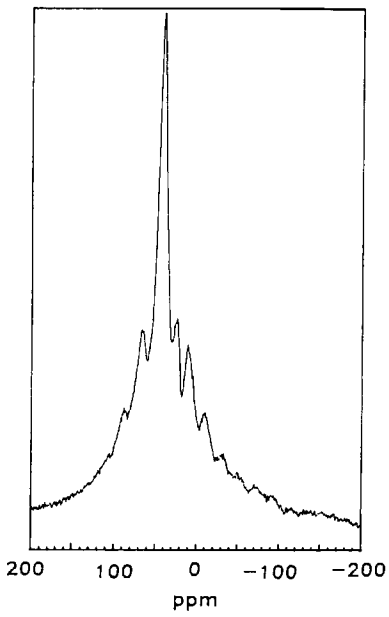

FIG. 6. ^{27}Al NMR spectra of 3A2B after calcination at 1000°C.

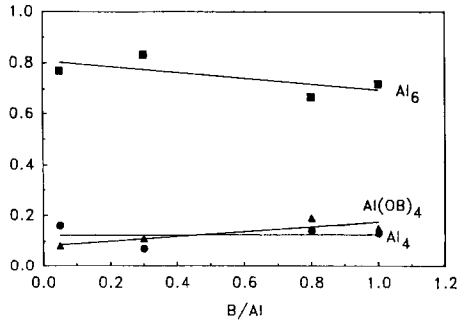

FIG. 7. Normalized concentrations of the ^{27}Al coordinations in the aluminum borates calcined at 500°C.

Figures 7 and 8 give the normalized integrated signals of the three aluminum coordinations from the various spectra of the materials calcined at 500 and 1000°C, respectively. For the 500°C calcined samples, all of the signals were relatively unaffected by any change in the B/Al ratio. For the 1000°C calcined samples there was a dramatic decrease in the AlO_6 concentration with a corresponding increase in the B/Al ratio. The concentration of $Al(OB)_4$ increased with increasing B/Al ratio. The AlO_4 concentration slightly increased with an increase in the calcination temperature but remained unaffected by increasing B/Al ratio.

Acidity

Previous reports have shown that alumina–boria catalysts can behave as acidic cracking catalysts (*1*, *22*). Reported alumina–boria catalysts differ from the aluminum borate catalysts described here mainly in their method of preparation (*22*).

Figure 9 summarizes the measurements of the relative strength of the acid sites and the concentration of acid sites as a function of the B/Al ratio. Values for the relative strength of the acid sites are expressed by the Hammett acidity function H_0. For the most acidic materials, the strength of the strongest sites were between H_0 of -3.3 and -8.7. The concentrations of acid sites reported are the total number of sites with $H_0 \leq +1.5$ (*8*).

The effect of boron on the relative strength of the acid sites was very pronounced. In going from pure alumina to an aluminum borate with a B/Al ratio of 0.05, the surface acid strength was seen to increase dramatically. Further increases in B content increased the acid strength, with a maximum strength quickly reached.

The effect of boron on the total concentration of acid sites is not as dramatic. Although there is significant scatter in the data, a general trend is seen toward increasing site concentration with boron. No distinction is made between Lewis or Brønsted acid sites with this titration method.

Reaction Studies

Table 3 summarizes the results of the 2-propanol dehydration study. The activation

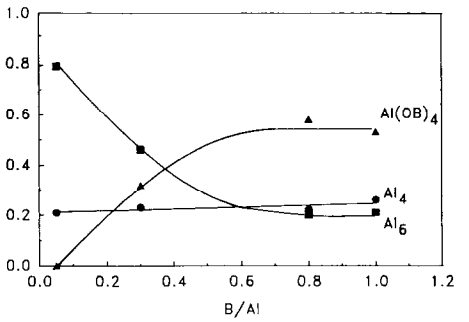

FIG. 8. Normalized concentrations of the ^{27}Al coordinations in the aluminum borates calcined at 1000°C.

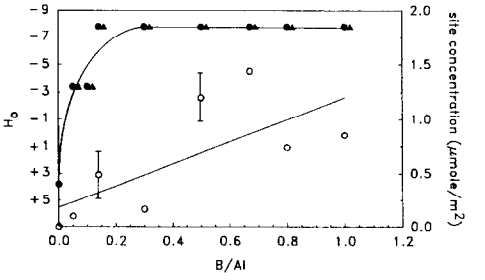

FIG. 9. Relative strength of acid sites: ●, 500°C calcined samples; ▲, 1000°C calcined samples; ○, concentration of acid sites with strength greater than an H_0 of +1.5. Lines are drawn for reference only.

TABLE 3

2-Propanol Conversions and Reaction Rates Calculated at 180°C

B/Al	E_a (kcal/mole)	% Conversion	Rate × 10^{-10} (mole/m²-sec)
0	30.3	0.4	0.02
0.05	25.2	3.4	0.15
0.3	21.2	2.5	0.11
0.5	26.1	8.2	0.49
0.67	28.8	5.1	0.33
1	27.2	3.8	0.22

energies listed are apparent activation energies as determined from Arrhenius plots. The apparent activation energies fall near the range of values given in the literature for 2-propanol dehydration (*23*).

The only reaction products observed over these catalysts were propylene and small amounts of oligomerization products, mainly C_6. No acetone was formed over any of the catalysts as would be expected in the presence of basic sites (*23*).

DISCUSSION

From the equilibrium phase diagram for the aluminum borate system (*24*), the dominant phase between temperatures of 300 and 2000°C and consisting of less than 10% B_2O_3 is expected to be the $9Al_2O_3 \cdot 2B_2O_3$ phase. This phase was not detected in any of the aluminum borates calcined at 500°C and only weak XRD signals of this phase were seen in samples calcined at 1000°C with a B/Al ≤ 0.3. This may be due in part to the preparation method employed in this study. Alternate synthesis methods given in the literature for aluminum borates involve the reaction of Al_2O_3 or $Al(OH)_3$ and B_2O_3 at high temperatures and pressures to give the borate phases $9Al_2O_3 \cdot 2B_2O_3$ and/or $2Al_2O_3 \cdot B_2O_3$ (*25*).

From the phase diagram, the dominant phase for materials consisting of more than 25% B_2O_3 between the temperatures of 500 and 1035°C is $2Al_2O_3 \cdot B_2O_3$. Three of the 1000°C calcined samples listed in Table 1 showed weak XRD signals corresponding to the $2Al_2O_3 \cdot B_2O_3$ and $9Al_2O_3 \cdot 2B_2O_3$ phases while four samples showed strong signals for $2Al_2O_3 \cdot B_2O_3$. It is interesting to note that $2Al_2O_3 \cdot B_2O_3$ only fully appeared in the aluminum borates which had a B/Al ratio greater than or equal to 0.5, which is equal to the B/Al ratio of the $2Al_2O_3 \cdot B_2O_3$ phase.

The suppression of formation of the γ-Al_2O_3 phase in the aluminum borates calcined at 500°C is evident from Table 1. All of the aluminum borates still maintained their amorphous quality after calcination at this temperature. In fact, no γ-Al_2O_3 was detected in any of these mixed oxides until 1000°C and none of the characteristic high-temperature phases of alumina, i.e., α-Al_2O_3 and θ-Al_2O_3, were seen in any of the aluminum borates.

This increase in thermal stability is not uncommon in mixed-alumina systems, where the presence of divalent ions or tetrahedral inclusions is known to result in increased thermal stability (*9*). This suggests the ability of tetrahedral boron to incorporate into the alumina structure, affecting the long-range order of the lattice. The observed results for the aluminum borates in Table 1 agree very well with the variation of thermal stability for other mixed-alumina systems such as alumina–aluminum phosphate (*2*).

As seen from the indicator and reaction studies, the inclusion of boron into the alumina structure also had a marked affect on the acidity. In many cases, acid strength can be closely related to catalytic activity, but the precise character of the dependence of reaction rate on acid strength varies from reaction to reaction (*23*). The dehydration of 2-propanol is not a very demanding reaction when it comes to acid strength. Even in pure Al_2O_3 some activity for dehydration of 2-propanol was evident at 180°C.

The high catalytic acidity of the aluminum borates is evident from the relatively high conversions of 2-propanol at 180°C. Under the reaction conditions employed

here, the temperatures normally reported for secondary alcohol dehydration range from 250 to 350°C (*23*). In this case, a few of the aluminum borate materials gave 100% conversion of the 2-propanol at temperatures as low as 250°C and a few of the materials even showed some activity at 130°C.

On the basis of the ^{11}B NMR studies, it is apparent that both trigonal and tetrahedral coordinated borons are present in aluminum borates. The relative amounts of the two coordinations are dependent on the B/Al ratio with the trigonal/tetrahedral ratio tending toward a value of 1/1 as the B/Al ratio increases. Figure 3 shows that the aluminum borate with a B/Al ratio of 1/20 calcined at 1000°C contained only tetrahedral coordination. This sample, along with the 1000°C calcined 10AB sample, not shown, were the only samples that lacked any trigonally coordinated boron. Also, these two samples were the only materials that from XRD indicated the presence of γ-Al_2O_3. Thus, it appears that trigonally coordinated boron can also inhibit the growth of crystalline γ-Al_2O_3 by incorporating itself into the alumina lattice and, due to its trigonal coordination, terminating any further lattice growth. When only tetrahedral boron coordination is present in a small amount, the disruption of the alumina lattice is not complete and some crystallinity can still exist.

The ^{27}Al NMR results showed the presence of three distinct Al signals which were assigned to AlO_4, AlO_6, and $Al(OB)_4$. It is curious as to why no $Al(OB)_x(OAl)_{4-x}$ (where $1 \leq x \leq 3$) was seen in any of the samples. The reason why these signals are not present is not clear but may be due to large quadrupolar interaction resulting in very broad and thus unobservable signals. On the other hand, the $Al(OB)_x(OAl)_{4-x}$ and $Al(OB)_4$ chemical shifts may be very close to one another and the different signals may overlap.

Table 2 reports the chemical shifts for each of the observed ^{27}Al coordinations and how they vary as a function of B/Al ratio and calcination temperature. The only signal which seems to be affected by calcination temperature is the $Al(OB)_4$ signal. Since the chemical shifts of both AlO_4 and AlO_6 are largely unaffected by calcination temperature, the same would be expected of $Al(OB)_4$. However, there is an approximate 15 ppm downfield shift of this signal with an increase in calcination temperature. The reason for a 15 ppm downfield shift of the $Al(OB)_4$ signal with an increase in calcination temperature is not clear but may be due to slight changes in the local environment affecting the quadrupolar coupling constant of the Al nucleus, thus resulting in a measurable change in chemical shift.

The relative amounts of the various Al coordinations shown in Fig. 7 show that the concentration of $Al(OB)_4$ increases with increasing boron content. This behavior is as expected since the more boron present, the more likely that direct Al–O–B would form.

Comparison of Figs. 4 and 9 show that there is a direct relationship between the acidity of these aluminum borates and the particular coordination of the boron atom. This relationship is more directly shown in Fig. 10. Such a dependence is predicted by a hypothesis advanced by Tanabe that the acid sites on binary metal oxides are formed by an excess of a positive or negative charge in the mixed oxides (*26*). Whether the charge is in excess or not and

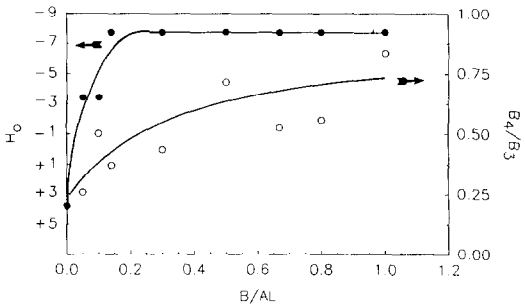

FIG. 10. Relation between boron–oxygen coordination and acid strength for the 500°C calcined samples.

whether it is positive or negative is determined in part by the coordination number of the minor cation, in this case, boron. This simple model predicts that tetrahedrally coordinated boron in an aluminum borate will result in an acidic material regardless of the coordination of aluminum.

There is a direct relation between the relative amounts of tetrahedral boron and the strength and concentration of acid sites for the 500°C calcined samples. For these materials, as the tetrahedral coordination increased, both the concentration of sites and the strength of sites increased. However, when comparing the boron coordination and strength of the acid sites for the 1000°C calcined samples, no such relationship seems to exist. The materials with corresponding B/Al ratios, regardless of their calcination temperature, exhibited the same relative acid strength. This is perhaps indicative of similarities in their surface structure as opposed to the differences observed by NMR and XRD in their bulk structure.

The nature of this acidity may be due to the electronegative properties of MO_x (where M = B or Al) groups. The acidity was seen to increase with an increase in the tetrahedral boron coordination. When the BO_4 coordination is compared to the BO_3 coordination, the additional oxygen may aid in the electron withdrawing (or proton donating) capabilities for the BO_4 coordination, thereby increasing the acidity and catalytic activity. When the BO_4 coordination is compared to the AlO_4 coordination, the higher electronegativity of boron may result in an increase in the surface acidity.

Comparison of Figs. 7 and 9 shows that there was no measurable relationship between the acidity of the 500°C calcined aluminum borates and the aluminum coordination. The relative concentrations of the various Al coordinations remained relatively constant as the strength and concentration of sites increased. This observation is in agreement with the simple acidity model proposed by Tanabe which predicts that the coordination of Al should have no affect on the acidity of aluminum borates.

From these results it is clear that boron is incorporating itself into the alumina lattice and dramatically affecting the acidity. What is interesting is that at 1000°C aluminum prefers the $Al(OB)_4$ to the AlO_6 coordination as the level of boron increases. This would help explain the absence of γ-Al_2O_3 in the samples with a B/Al ratio greater than 0.10. A concentration level at which there is not enough AlO_6 present for γ-Al_2O_3 to form is reached.

In conclusion, the high acidity and catalytic activity of these aluminum borate mixed oxides can be attributed to the inclusion of tetrahedral boron into the alumina lattice. The inclusion of tetrahedral boron into the alumina lattice also increases the thermal stability. The concentration of tetrahedral boron is a function of the stoichiometry and the temperature of calcination. Therefore, the concentration of tetrahedral boron, and thus the acidity and catalytic activity, can perhaps be controlled by proper tuning of the preparation parameters.

ACKNOWLEDGMENTS

The authors acknowledge financial support for this work from the National Science Foundation under Grant CPE-8511788 and the Office of Naval Research under Grant N00014-85-G-0087.

REFERENCES

1. Tanabe, K., "Solid Acids and Bases." Academic Press, New York, 1970.
2. Mitchell, S. F., Marcelin, G., and Goodwin, J. G., Jr., *J. Catal.* **105,** 521 (1987).
3. Moffat, J. B., *Catal. Rev. Sci. Eng.* **18,** 199 (1978).
4. Gates, B. C., Katzer, J. R., and Schuit, G. C., "Chemistry of Catalytic Processes." McGraw–Hill, New York, 1979.
5. Delanny, F., "Characterization of Heterogeneous Catalysts." Dekker, New York, 1984.
6. Benesi, H. A., *J. Amer. Chem. Soc.* **78,** 5490 (1956).
7. Benesi, H. A., *J. Phys. Chem.* **61,** 970 (1957).
8. Hammett, L. P., and Deyrup, A. J., *J. Amer. Chem. Soc.* **54,** 2721 (1932).
9. Marcelin, G., Vogel, R. F., and Kehl, W. L., *Appl. Catal.* **12,** 237 (1984).
10. Yamaguchi, O., Tada, M., Takeoka, K., and

Shimizu, K., *Bull. Chem. Soc. Japan* **52,** 2153 (1979).
11. Turner, G., Smith, K., Kirkpatrick, R., and Oldfield, E., *J. Magn. Reson.* **67,** 544 (1986).
12. Bray, P. J., Edwards, J. O., O'Keefe, J. G., Ross, V. F., and Tatsuzaki, I., *J. Chem. Phys.* **35,** 435 (1961).
13. Kriz, H. M., Bishop, S. B., and Bray, P. J., *J. Chem. Phys.* **49,** 557 (1968).
14. Lai, K. C., and Petch, H. E., *J. Chem. Phys.* **43,** 178 (1965).
15. Alemany, L. B., and Kirker, G. W., *J. Amer. Chem. Soc.* **108,** 6158 (1986).
16. Muller, D., Gessner, W., Behrens, H. J., and Scheler, G., *Chem. Phys. Lett.* **79,** 59 (1981).
17. Lippmaa, E., Samoson, A., and Magi, M., *J. Amer. Chem. Soc.* **108,** 1730 (1986).
18. Oestrike, R., Navrotsky, A., Turner, G. L., Montez, B., and Kirkpatrick, R. J., *Amer. Mineral.* **72,** 788 (1987).
19. Dupree, R., Holland, D., and Williams, D. S., *Phys. Chem. Glasses* **26,** 50 (1985).
20. Risbud, S. H., Kirkpatrick, R. J., Taglialavore, A. P., and Montez, B., *J. Amer. Ceram. Soc.* **70,** C10 (1987).
21. Dupree, R., Farnan, I., Forty, A. J., El-Mashri, S., and Bottyan, L., *J. Phys.* **46,** C8 (1985).
22. Izumi, Y., and Shiba, T., *Bull. Chem. Soc. Japan* **37,** 1797 (1964).
23. Kibby, C. L., and Hall, W. K., *J. Catal.* **29,** 144 (1973).
24. Gielisse, P. J. M., and Foster, W. R., *Nature (London)* **195**[4836], 70 (1962).
25. Bither, T. A., and Young, H. S., *J. Solid State Chem.* **6,** 502 (1973).
26. Tanabe, K., Sumiyoshi, T., Shibata, K., Kiyoura, T., and Kitagawa, J., *Bull. Chem. Soc. Japan* **47,** 1064 (1974).